

as sulfide and the other two represent thiolate-like and an oxidized sulfur species.

3. The sulfur K-edge features of the oxidized sulfur species on FeMo-co show close correspondence with those of bound thiosulfate. From the relative intensities of the various spectral features, it seems likely that at least one, or possibly more,  $S_2O_3$ -like moieties are bound. The presence of this anion as ligand may account for the overall negative charge of FeMo-co.<sup>6</sup> The presence of this ligand can also explain the thiolate-like feature in the XANES spectrum.

4. Chloride plays no part in ligation of iron or molybdenum in intact FeMo-co(ox).

5. The Mo atom is surrounded by a mixed sulfur and oxygen ligation sphere disposed in a distorted-octahedral manner. The close spectral correlation with the Mo–Fe–S dicubane clusters suggests a similar oxidation state for molybdenum, which may be best described as 4+ when recent ENDOR results are also considered.<sup>39,40</sup>

6. Comparison of the molybdenum L edges of both the oxidized and semireduced states of FeMo-co clearly shows the oxidation state of molybdenum is unchanged (at least within a small fraction of an electron) in this redox reaction.

7. Solutions of dithionite-free FeMo-co are stable in solution to X-ray-induced photoreduction. In contrast, solutions of FeMo-co(ox) containing dithionite-derived products (as well as chloride and possibly other unidentified molecules) completely photoreduce under the conditions of the XANES experiment within about 12 h.

As a result of these studies several major questions arise.

What is the source of the  $S_2O_3^{2-}$ ? The simplest explanation is that it is produced during “self-oxidation” of FeMo-co, via the well-known disproportionation of  $S_2O_4^{2-}$  into  $S_2O_3^{2-}$  and  $HSO_3^-$ .<sup>42</sup>

However, the possibility remains that the  $S_2O_3^{2-}$  could derive from a novel ligand type intrinsic to the MoFe protein.

Is the unique ability of dithionite-containing NMF solutions to extract FeMo-co from the MoFe protein due to the presence of  $S_2O_3^{2-}$  acting as a ligand? If so, then is dithionite itself necessary as a reductant? This situation could rationalize the recent extraction of FeMo-co into DMF or MeCN but only in the presence of  $(Et_4N)_2S_2O_4$ .<sup>43</sup> The  $Et_4N^+$  salt of dithionite was noted as being particularly unstable in these solutions, suggesting the formation of considerable  $S_2O_3^{2-}$ .

Finally, if molybdenum is to play a major role in dinitrogen binding and reduction, why does it not receive the electron in the oxidized to semireduced reduction? Molybdenum must be included in subsequent electron transfers for the binding of the weakly  $\pi$ -acid dinitrogen molecule to be effective. Possibly then, the production of the sustained reducing (red) state involves electron transfer to molybdenum aided by energy-dependent conformational changes within the MoFe protein (driven by, e.g., interaction with the iron protein–ATP complex).

**Acknowledgment.** This work was supported by the National Science Foundation through Grant CHE 85-12129 to K.O.H. and by the National Institutes of Health through Grants RR1209 to K.O.H. and DK-37255 to W.E.N. Stanford Synchrotron Radiation Laboratory is supported by the Department of Energy, Office of Basic Energy Sciences, and the National Institutes of Health, Division of Research Resources.

(42) Danehy, J. P.; Zubritsky, C. W. III *Anal. Chem.* **1974**, *46*, 391. Cermák, V.; Smutek, M. *Collect. Czech. Chem. Commun.* **1975**, *40*, 3241. Kilroy, W. P. *J. Inorg. Nucl. Chem.* **1979**, *42*, 1071.

(43) Lough, S. M.; Jacobs, D. L.; Lyons, D. L.; Watt, G. D.; McDonald, J. W. *Biochem. Biophys. Res. Commun.* **1986**, *139*, 740.

## NMR Study of the Conformations of Free and Lanthanide-Complexed Glutathione in Aqueous Solution

Benjamin Podányi and R. Stephen Reid\*

Contribution from the Department of Chemistry, University of Saskatchewan, Saskatoon, Saskatchewan S7N 0W0, Canada. Received July 30, 1987

**Abstract:** The  $^1H$  and  $^{13}C$  NMR spectra of glutathione in its free and La(III)-complexed forms have been analyzed. The vicinal coupling constants were used to gain rotamer populations by the Karplus approach. The data were compared with the results of previous X-ray crystallographic, theoretical, and NMR studies. The gadolinium(III) complex of glutathione has been studied by the measurement of Gd(III)-induced  $^1H$  and  $^{13}C$  spin–lattice relaxation rate enhancements and application of the Solomon–Bloembergen equation. The two carboxylate groups of the molecule are found to be competing complexation sites; the microscopic formation constants have been determined. Complexation to the lanthanide(III) ions does not appear to change the conformational equilibrium of glutathione substantially.

Gadolinium(III) complexes are now widely used as “contrast agents” in nuclear magnetic resonance imaging.<sup>1</sup> An understanding of the specific relaxation rate enhancement of these paramagnetic complexes in different tissues, and of their toxicity, requires a detailed investigation of the behavior of Gd(III) complexes with biologically relevant molecules. We have therefore instituted a study of the stability and structure of such complexes in aqueous solution. The previous paper in this series<sup>2</sup> investigated the structure of amino acid and lactic acid complexes of Gd(III) using  $^1H$  NMR relaxation rate enhancement measurements.

The present study concerns the Gd(III) complex of the tripeptide glutathione ( $\gamma$ -glutamylcysteinylglycine, GSH). GSH

is a constituent of most cells, with several biochemical functions.<sup>3</sup> It is present at a concentration suitable for convenient NMR observation in vivo (for example, at approximately 2 mM in the human erythrocyte<sup>4,5</sup>). It possesses several potential metal-complexing sites. To our knowledge, no study of the Gd(III) complex has so far been reported in the literature.

We also consider here the solution conformations of free GSH. The conformation in the solid has been established by X-ray crystallography,<sup>6</sup> and possible conformations have also been

(3) Larsson, A.; Orrhenius, S.; Holmgrew, A.; Mannervik, B. *Functions of Glutathione*; Raven: New York, 1983.

(4) Ibbott, F. A. In *Clinical Chemistry*; Henry, R. J., Cannon, D. C.; Winkelman, J. W., Eds.; Harper and Row: New York, 1974; p 618.

(5) Brown, F. F.; Campbell, I. D.; Kuchel, P. W.; Rabenstein, D. L. *FEBS Lett.* **1977**, *82*, 12.

(1) Carr, D. H. *Physiol. Chem. Phys. Med. NMR* **1985**, *16*, 137.

(2) Reid, R. S.; Podányi, B. *Can. J. Chem.* **1987**, *65*, 1508–1512.

predicted by theoretical methods.<sup>7,8</sup> The molecule has been the subject of several solution studies by NMR spectroscopy. Microscopic acid-dissociation constants were determined by exploitation of the pH dependence of <sup>1</sup>H and <sup>13</sup>C NMR spectra.<sup>9,10</sup> Uncertainties in the <sup>13</sup>C assignments were resolved using deuterium isotope effects<sup>11</sup> and later by 2D NMR methods.<sup>12</sup> <sup>15</sup>N NMR chemical shifts and coupling constants in aqueous solution have also been reported,<sup>13</sup> and the exchange rate between solvent and amide protons in aqueous solution has been measured.<sup>14</sup>

Only three reports have appeared concerning the investigation by NMR of the conformation(s) of GSH in solution.<sup>15-17</sup> The conclusions of Zenin et al.,<sup>15</sup> based upon pH trends in chemical shifts, are unwarranted because no account was taken of the effect of microscopic acid dissociation upon the situation. The study of Fujiwara et al.,<sup>16</sup> based upon Karplus analysis of vicinal <sup>1</sup>H-<sup>1</sup>H coupling constants derived from second-order spectral analysis, was performed at 2.3 T; because of the consequently poor dispersion, the authors could determine unambiguously the rotamer populations around only one bond. A similar study was performed more recently by York et al.<sup>17</sup> at 9.4 T; however, because rotamer populations around several bonds were still not determined, support for the predominance of particular conformations was based on more circumstantial evidence, such as the temperature dependence of amide proton chemical shifts and <sup>13</sup>C T<sub>1</sub> and nonselective NOE measurements.

We therefore judged it useful to investigate this area more thoroughly. The present study includes as complete as possible an analysis of the <sup>1</sup>H spectrum, to yield <sup>1</sup>H-<sup>1</sup>H vicinal couplings, including those involving amide protons. Karplus-type analysis then yields direct conformational information for all salient bonds in the molecule save one (see below), using also three-bond <sup>13</sup>C-<sup>1</sup>H coupling constant information to resolve some ambiguities.

Generally, a vicinal coupling constant involving two protons attached to atoms connected by a bond with free torsional motion is determined by eq 1, where  $\phi$  is the torsion angle,  $P(\phi)$  is the

$$J = \int P(\phi) J(\phi) d\phi \quad (1)$$

population function of the conformations characterized by different torsion angles, determined by the energy of the conformations via the Boltzmann equation, and  $J(\phi)$  is the coupling constant as a function of the torsion angle. In practical applications this integral can be estimated by the discrete summation of a definite number of cases, most frequently the three rotamers where the two protons under consideration are staggered (eq 2) where  $p_I$ ,  $p_{II}$ , and  $p_{III}$

$$J = p_I J_I + p_{II} J_{II} + p_{III} J_{III} \quad (2)$$

are the populations of the three rotamers and  $J_I$  and  $J_{II}$  are the coupling constants for the trans and gauche arrangements, respectively, of the protons. Bearing in mind that by definition  $p_I + p_{II} + p_{III} = 1$ , measurement of two coupling constants across one bond enables estimation of the rotamer populations.

In the case of GSH complexed partially by Gd(III), the distance from the Gd(III) ion to a given proton can be estimated also by calculating relaxation times in the complex and then applying the Solomon-Bloembergen equation.<sup>18</sup> The details of this method,

**Table I.** <sup>1</sup>H NMR Chemical Shifts (ppm) of Glutathione in D<sub>2</sub>O

assignt	0.05 M GSH	1.0 M GSH	0.05 M GSH + 0.1 M La(NO <sub>3</sub> ) <sub>3</sub>
Gly α-H <sub>2</sub>	3.79	3.80	3.80
Gly NH	8.27 <sup>a</sup>		8.25 <sup>a</sup>
Cys α-H	4.56	4.56	4.55
Cys β-H <sub>a</sub>	2.92	2.92	2.92
Cys β-H <sub>b</sub>	2.95	2.96	2.96
Cys NH	8.48 <sup>a</sup>		8.41 <sup>a</sup>
Glu γ-H <sub>a</sub>	2.53	2.53	2.54
Glu γ-H <sub>b</sub>	2.55	2.57	2.57
Glu β-H <sub>2</sub>	2.15	2.16	2.17
Glu α-H	3.77	3.79	3.80

<sup>a</sup> Measured in H<sub>2</sub>O/10% D<sub>2</sub>O.

**Table II.** <sup>1</sup>H NMR Coupling Constants of Glutathione in D<sub>2</sub>O<sup>a</sup>

assignt	0.05 M GSH	1.0 M GSH	0.05 M GSH + 0.1 M La(NO <sub>3</sub> ) <sub>3</sub>
<sup>2</sup> J <sub>Gly α-H<sub>a</sub>, Gly α-H<sub>b</sub></sub>			-17.5 ± 0.1
<sup>3</sup> J <sub>Gly α-H<sub>a</sub>, NH</sub> + <sup>3</sup> J <sub>Gly α-H<sub>b</sub>, NH</sub>	11.7 ± 0.1 <sup>c</sup>		11.5 ± 0.1 <sup>c</sup>
<sup>3</sup> J <sub>Cys α-H, Cys β-H<sub>a</sub></sub>	7.3 ± 0.1	7.2 ± 0.1	7.3 ± 0.1
<sup>3</sup> J <sub>Cys α-H, Cys β-H<sub>b</sub></sub>	4.9 ± 0.1	5.0 ± 0.1	5.1 ± 0.1
<sup>2</sup> J <sub>Cys β-H<sub>a</sub>, Cys β-H<sub>b</sub></sub>	-14.3 ± 0.1	-14.0 ± 0.1	-14.1 ± 0.1
<sup>3</sup> J <sub>Cys α-H, NH</sub>	7.5 ± 0.1 <sup>c</sup>		7.5 ± 0.1 <sup>c</sup>
<sup>2</sup> J <sub>Glu γ-H<sub>a</sub>, Glu γ-H<sub>b</sub></sub>	-15.3 ± 0.1	-15.5 ± 0.1	-15.6 ± 0.1
<sup>3</sup> J <sub>Glu γ-H<sub>a</sub>, Glu β-H<sub>a</sub></sub>	8.5 ± 0.2	8.3 ± 0.5	8.1 ± 0.3
<sup>3</sup> J <sub>Glu γ-H<sub>a</sub>, Glu β-H<sub>b</sub></sub>	6.8 ± 0.2	7.0 ± 0.4	6.8 ± 0.3
<sup>3</sup> J <sub>Glu β-H<sub>a</sub>, α-H</sub> + <sup>3</sup> J <sub>Glu β-H<sub>b</sub>, α-H</sub>	12.8 ± 0.1	12.8 ± 0.1	12.8 ± 0.2

<sup>a</sup> In hertz. <sup>b</sup> Standard deviations are those estimated from spectral analysis. <sup>c</sup> Measured in H<sub>2</sub>O/10% D<sub>2</sub>O.

and the inherent assumptions, have been previously discussed.<sup>2</sup> It is then possible to compare free and complexed solution structures with each other and with theoretically predicted and solid-state structures.

## Experimental Section

**Chemicals.** Reduced glutathione, lanthanum nitrate (Aldrich), and gadolinium nitrate (Alfa Products) were used as received.

**Preparation of Solutions.** All measurements were made at pH\* 4.6. The pH\* was measured with a Beckman SS-2 pH meter equipped with a glass combination electrode and calibrated in the usual manner. The pH\* was adjusted by adding DCl or NaOD to the solution. All samples were flushed with nitrogen and degassed by sonication to prevent oxidation of glutathione by dissolved oxygen. No NMR signals ascribable to oxidized glutathione were observed. Spectra of the free GSH were collected at concentrations of 0.05 and 1.0 M in D<sub>2</sub>O and in 10% D<sub>2</sub>O/90% H<sub>2</sub>O, using DSS as a chemical shift reference. Spectra of La(III)-complexed glutathione were recorded at 0.05 M GSH. For experiments involving Gd(III), different Gd(III) concentrations were achieved by the successive addition of small volumes (3.5-4.5 μL) of a stock D<sub>2</sub>O solution 0.001 or 0.01 M in Gd(NO<sub>3</sub>)<sub>3</sub> to 0.02 M (<sup>1</sup>H NMR) or 1 M (<sup>13</sup>C NMR) ligand solutions. The exact amount added was determined by weight. The absence of measurable outer-sphere relaxation effects was established with a sample containing additional tetra-*n*-butylammonium bromide.

**NMR Measurements.** All NMR spectra were collected on a Bruker AM-300 spectrometer at a probe temperature of 30 ± 1 °C. Proton spectra in 10% D<sub>2</sub>O were collected with a 1331 binomial composite pulse<sup>19</sup> to suppress the water signal. Spin-lattice relaxation times were measured by the standard inversion-recovery method, with 10-12 different delay values. For <sup>13</sup>C T<sub>1</sub> measurements, a composite inverting pulse<sup>20</sup> was used, and separate measurements were performed for the aliphatic and the carbonyl signals. Gd(III) ion induced line broadenings were corrected for variations in field homogeneity using the DSS methyl signal line width.

**Calculations.** Spectral parameters were extracted from the second-order <sup>1</sup>H spectra using the Bruker routine PANIC. Relaxation times were calculated by the standard Bruker routine and checked by weighted linear least-squares analysis. Relative standard deviations of the resultant T<sub>1</sub>

- (6) Wright, W. B. *Acta Crystallogr.* **1958**, *11*, 632.  
 (7) Laurence, P. R.; Thomson, C. *Theor. Chim. Acta* **1980**, *57*, 25-41.  
 (8) Sandalova, T. P.; Belobrov, P. I. *Bioorg. Khim.* **1983**, *9*, 1013-1020.  
 (9) Rabenstein, D. L. *J. Am. Chem. Soc.* **1973**, *95*, 2797-2803.  
 (10) Jung, G.; Breitmaier, E.; Voelter, W. *Eur. J. Biochem.* **1972**, *24*, 438-445.  
 (11) Feeney, J.; Partington, P.; Roberts, G. C. K. *J. Magn. Reson.* **1974**, *13*, 268-274.  
 (12) (a) Huckerby, T. N.; Tutor, A. J.; Dawber, J. G. *J. Chem. Soc., Perkin Trans. 2* **1985**, 759-763. (b) Haslinger, E.; Robien, W. *Mol. Cryst. Liq. Cryst.* **1985**, *116*, 137-139.  
 (13) Marchal, J. P.; Canet, D. *Biochemistry* **1980**, *19*, 1301-1304.  
 (14) Schwartz, A. L.; Cutnell, J. D. *J. Magn. Reson.* **1983**, *53*, 398-411.  
 (15) Zenin, S. V.; Chuprina, G. I.; Krylova, A. Yu. *J. Gen. Chem. USSR (Engl. Transl.)* **1975**, *45*, 1309-1311.  
 (16) Fujiwara, S.; Formicka-Kozłowska, G.; Kozłowski, H. *Bull. Chem. Soc. Jpn.* **1977**, *50*, 3131-3135.  
 (17) York, M. J.; Beilharz, G. R.; Kuchel, P. W. *Int. J. Pept. Protein Res.* **1987**, *29*, 638-646.

- (18) (a) Solomon, I. *Phys. Rev.* **1959**, *99*, 559. (b) Bloembergen, N. *J. Chem. Phys.* **1957**, *27*, 572.  
 (19) Hore, P. J. *J. Magn. Reson.* **1983**, *55*, 283-300.  
 (20) Levitt, M. H.; Freeman, R. *J. Magn. Reson.* **1979**, *33*, 473.

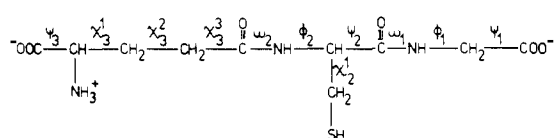


Figure 1. Labeling of the torsion angles of glutathione.

Table III.  $^{13}\text{C}$  NMR Chemical Shifts (ppm) of Glutathione in  $\text{D}_2\text{O}$ 

assignt	0.05 M GSH	1.0 M GSH	0.05 M GSH + 0.1 M $\text{La}(\text{NO}_3)_3$	0.05 M GSH + 0.12 mM $\text{Gd}(\text{NO}_3)_3^a$
Gly COO	178.6	178.5	180.3	178.8 (22)
Gly $\alpha$ -C	45.8	45.8	46.1	45.6 (10)
Cys CON	174.4	174.3	174.6	174.4 (1)
Cys $\alpha$ -C	58.3	58.2	58.4	58.3 (0)
Cys $\beta$ -C	28.2	28.2	28.1	28.2 (0)
Glu CON	177.7	177.4	177.7	177.7 (1)
Glu $\gamma$ -C	34.1	34.0	33.8	34.1 (0)
Glu $\beta$ -C	28.8	28.8	28.7	28.8 (0)
Glu $\alpha$ -C	56.8	56.7	56.7	56.8 (3)
Glu COO	176.6	176.5	177.2	176.6 (5)

<sup>a</sup>The Gd(III)-induced line broadening of the signal in parentheses (hertz).

Table IV.  $^{13}\text{C}$  NMR Coupling Constants of Glutathione in  $\text{D}_2\text{O}^a$ 

assignt	0.05 M GSH	0.05 M GSH + 0.1 M $\text{La}(\text{NO}_3)_3$
$^1J_{\text{Gly } \alpha\text{-C}}$	139.5	139.8
$^1J_{\text{Cys } \alpha\text{-C}}$	142.9	143.3
$^1J_{\text{Cys } \beta\text{-C}}$	144.0	143.2
$^1J_{\text{Glu } \gamma\text{-C}}$	128.7	
$^1J_{\text{Glu } \beta\text{-C}}$	131.4	
$^1J_{\text{Glu } \alpha\text{-C}}$	145.7	145.8
$^2J_{\text{Gly COO, Gly } \alpha\text{-H}}$	5.2	5.4
$^2J_{\text{Cys } \beta\text{-C, Cys } \alpha\text{-H}}$	5.1	4.5
$^3J_{\text{Glu } \gamma\text{-C, Glu } \alpha\text{-H}}$	4.5	
$^3J_{\text{Glu } \alpha\text{-C, Glu } \gamma\text{-H}_a} + ^3J_{\text{Glu } \alpha\text{-C, Glu } \gamma\text{-H}_b}$	8.4	9.0
$^2J_{\text{Glu COO, Glu } \alpha\text{-H}}$	4.9	4.5
$^3J_{\text{Glu COO, Glu } \beta\text{-H}_a} + ^3J_{\text{Glu COO, Glu } \beta\text{-H}_b}$	7.6	8.0

<sup>a</sup>In hertz.

values were less than  $\pm 5\%$  in all cases. The distances between Gd(III) ions and the carbons and hydrogens of the glutathione molecule in different conformations were calculated by the MMS program<sup>21</sup> of the IRIS system on a Silicon Graphics terminal using the X-ray coordinates of free glutathione<sup>6</sup> as input data. Expressions for fractional complexation values as a function of microscopic formation constants and total metal and ligand concentrations were obtained by solving the system of equilibrium and mass-balance equations with the routine MAPLE.<sup>22</sup> The nonlinear regression fit of the measured and calculated fractional complexation values was performed with MINPACK.<sup>23</sup> MAPLE and MINPACK calculations were performed on a DEC VAX 8600 computer.

## Results

**Free Glutathione.** Tables I–IV summarize the assignments, chemical shifts, and coupling constants recorded. Individual carbons are labeled by residue and by position relative to the carboxyl/amino carbon. Torsion angles are labeled according to internationally accepted nomenclature,<sup>24</sup> as shown in Figure 1. The coupling constant data are used below to attempt to gain the rotamer populations around the 11 labeled bonds.

**Torsion Angles  $\Psi_1$  and  $\phi_1$ .** Theoretical calculations of the conformational energy around these bonds in glutathione ionized at both carboxylate groups<sup>7</sup> predicted that one conformation, having a five-membered ring stabilized by hydrogen bonding between the amide NH and one of the carboxylate oxygens, would have a much lower energy than all other forms. In this confor-

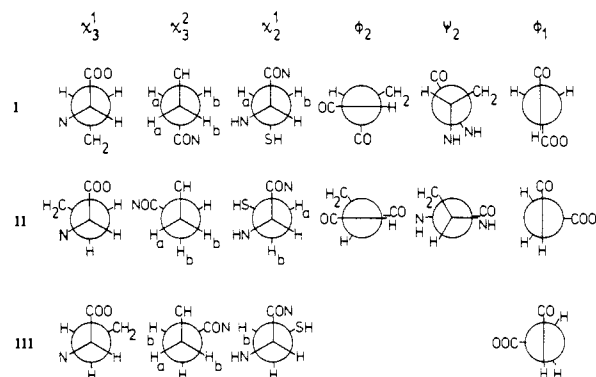


Figure 2. Newman projections of the stable rotamers of glutathione. See text for explanations.

Table V. Rotamer Populations around the Bonds of Glutathione (%)

bond	$P_I$	$P_{II}$	$P_{III}$
$\phi_1$ and $\Psi_1$	36	32	32
$\phi_2$ and $\Psi_2$	75	25	
$\chi_2^1$	49	31	20
$\chi_3^2$	40	30	30
$\chi_3^1$	44	23	33

mation both  $\Psi$  and  $\phi$  are  $180^\circ$ . According to the described torsion angle dependence of the sum of  $^3J_{\text{CH}_a\text{NH}}$  and  $^3J_{\text{CH}_b\text{NH}}$  in glycine derivatives,<sup>25</sup> this value would be 6.7 Hz in this conformer. However, the measured value is 11.7 Hz, indicating that in aqueous solution other conformations must be also considered. On steric grounds, conformations characterized by  $\phi = 0^\circ$  probably have much higher energy; however, several other conformations are possible. With respect to the  $^3J_{\text{CH}_b\text{NH}}$  coupling constants, the averages of these are the forms with  $\phi = \pm 90^\circ$ , shown in Figure 2. In these forms the sum of the two vicinal coupling constants should be 14.5 Hz.<sup>25</sup> The resultant rotamer populations are given in Table V.

**Torsion Angles  $\omega_1$  and  $\omega_2$ .** It has been shown that values of  $^1J_{\text{N,H}}$  in excess of 92 Hz are characteristic for the *trans*-amide linkage.<sup>25</sup> The reported values in aqueous solution for these couplings<sup>13</sup> are well above this limit, so both torsion angles are  $180^\circ$ . This is as expected for a linear peptide.

**Torsion Angles  $\phi_2$  and  $\Psi_2$ .** The complete energy map is available in the literature around these bonds,<sup>7</sup> and the torsion angle dependence of  $^3J_{\alpha\text{-H,NH}}$  in peptides is also well documented,<sup>25</sup> so this coupling constant can be calculated according to eq 1, approximating the integral by a summation of  $10^\circ$  steps around both torsion angles. The value of this coupling constant thus obtained (8.4 Hz) is somewhat higher than the measured value (7.3 Hz). Both theoretical studies<sup>7,8</sup> predict that, for the conformer of lowest energy,  $\phi_2 = -90^\circ$  and  $\Psi_2 = -30^\circ$ , in close agreement with the crystal structure.<sup>6</sup> The published conformational map shows another minimum at the extended conformation ( $\phi = 180^\circ$ ;  $\Psi = 180^\circ$ ). A simplified interpretation of the measured coupling constant can be made by assuming equilibrium of the above-mentioned two conformations (Figure 2). The populations summarized in Table V were calculated using values for the coupling constants of 8.8 and 3.5 Hz, respectively.<sup>25</sup>

**Torsion Angle  $\chi_2^1$ .** The conformational equilibrium around this bond can be interpreted in terms of the three staggered conformations (Figure 2) and the rotamer population calculated according to eq 2. The assignment of the two diastereotopic  $\beta$ -H's is based on the chemical shift difference reported in the literature for a peptide stereoselectivity deuterated at the cysteine  $\beta$ -H.<sup>26</sup> Coupling constants for the individual rotamers were calculated from an extended Karplus-type equation that allows for substituent

(21) Dempsey, S., The UCSD Molecular Modeling System, University of California, San Diego, CA, 1985.

(22) Chan, B. W.; Geddes, K. O.; Eonnet, G. H.; Watt, S. M. *Maple User's Guide*; Watcom: Waterloo, 1985.

(23) MINPACK-1 Fortran Program, Argonne National Laboratory Report No. AN-80-74, 1974.

(24) IUPAC-IUB Commission on Biochemical Nomenclature *J. Mol. Biol.* **1970**, *52*, 1; *Biochemistry* **1970**, *9*, 3471.

(25) Bystrov, V. F. In *Progress in NMR Spectroscopy*; Emsley, J. W., Feeney, J., Sutcliffe, L. H., Eds. Pergamon: Oxford, U.K., 1976; Vol. 10, p 41.

(26) Fischman, A. J.; Live, D. H.; Wyssbrod, H. R.; Agosta, W. C.; Cowburn, D. *J. Am. Chem. Soc.* **1980**, *102*, 2533–2539.

inductive effects.<sup>27</sup> Rotamer populations are summarized in Table V.

**Torsion Angle  $\chi^2_3$ .** The conformational equilibrium around this bond can be interpreted in terms of the three staggered conformations (Figure 2). It is assumed that II and III are of equal energy. The rotamer population can then be estimated from three different coupling constants:  $^3J_{\gamma\text{-H}_a,\beta\text{-H}_a}$ ,  $^3J_{\gamma\text{-H}_a,\beta\text{-H}_b}$ , or  $(^3J_{\alpha\text{-C},\gamma\text{-H}_a} + ^3J_{\alpha\text{-C},\gamma\text{-H}_b})$ . As standard proton-proton vicinal trans and gauche couplings, 13.5 and 2.8 Hz were used.<sup>27</sup> Values of 10 and 1.2 Hz were used for the corresponding carbon-proton coupling constants.<sup>28</sup> The estimated populations for rotamer II are 23, 37, and 30%, respectively. The median value is given in Table V.

**Torsion Angle  $\chi^1_3$ .** The conformational equilibrium around this bond can be interpreted by the three staggered conformations, shown in Figure 2. The two  $\beta$ -protons have the same chemical shift in the spectrum, so the populations of the three rotamers can be calculated only by the combined application of the vicinal proton-proton and carbon-proton coupling constants, according to the procedure first described by Hansen et al.<sup>29</sup> The population of rotamer I can be calculated from the carbon-proton coupling constants according to eq 3, where  $(J_{A,X} + J_{B,X})$  is the measured

$$p = [J_g + J_i - (J_{A,X} + J_{B,X})] / (J_i - J_g) \quad (3)$$

value of  $(J_{\text{COO},\beta\text{-H}_a} + J_{\text{COO},\beta\text{-H}_b})$ . The standard trans and gauche coupling constants for this band are taken to be 11 and 1 Hz, respectively, after Hansen et al.<sup>29</sup> The population of rotamer II can be calculated from the proton-proton coupling constant according to eq 3, where  $(J_{A,X} + J_{B,X})$  is now the measured value of  $(J_{\beta\text{-H}_a,\alpha\text{-H}} + J_{\beta\text{-H}_b,\alpha\text{-H}})$ , and the standard trans and gauche coupling constants are assumed to be 13 and 3 Hz, respectively.<sup>25</sup> The calculated rotamer populations are summarized in Table V.

No unambiguous information about the torsion angles  $\Psi_3$  and  $\chi^3_3$  can be extracted from the measured coupling constants. (In principle,  $^3J_{\gamma\text{-H}_a,\text{N}}$  and  $^3J_{\gamma\text{-H}_b,\text{N}}$  could supply information regarding  $\chi^3_3$ ,<sup>30</sup> we are currently investigating this possibility). For all the proton-proton coupling constants, no statistically significant differences were observed between the values measured at two very different concentrations (Table II).

**Complexed Glutathione.** Because of the heavily paramagnetic nature of the gadolinium(III) ion, no coupling constants can be measured in the stoichiometric Gd(III)-glutathione complex, due to the extreme line broadening engendered. However, it has been shown that some amino acids form isostructural complexes with all the lanthanide elements,<sup>31</sup> and this has been previously assumed to apply also to peptide complexes of lanthanides.<sup>32</sup> We therefore collected the  $^1\text{H}$  and  $^{13}\text{C}$  spectra of GSH in aqueous solutions containing lanthanum(III) (the only nonparamagnetic lanthanide ion). A twofold excess of La(III) was used, because, according to the known formation constants of the 1:1 GSH-La(III) complex,<sup>33</sup> a substantial amount of the GSH is complexed at this concentration. Results are summarized in Tables I-IV. There are no significant changes in the coupling constants or in the  $^1\text{H}$  chemical shifts relative to free glutathione, and only the carboxylate carbons show a significant increase in  $^{13}\text{C}$  chemical shift (+1.7 ppm for the glycine residue; +0.6 ppm for the glutamic acid). This suggests that the complexation sites of the glutathione molecule are the two carboxylate end groups only. The coupling constant data indicate that complexation appears to change the conformational status of the molecule very little. As discussed

(27) Haasnoot, C. A. G.; De Leeuw, F. A. A. M.; Altona, C. *Tetrahedron* **1980**, *36*, 2783-2792.

(28) Marshall, J. L. *Carbon-carbon and Carbon-proton NMR Couplings*; Verlag Chemie International: Deerfield Beach, FL, 1983.

(29) Hansen, P. E.; Feeney, J.; Roberts, G. C. K. *J. Magn. Reson.* **1975**, *17*, 249-261.

(30) Levy, G. C.; Lichter, R. L. *Nitrogen-15 Nuclear Magnetic Resonance Spectroscopy*; Wiley: New York, 1979; p 117.

(31) (a) Elgavish, G. A.; Reuben, J. *J. Am. Chem. Soc.* **1978**, *100*, 3617.

(b) Elgavish, G. A.; Reuben, J. *J. Magn. Reson.* **1981**, *42*, 242.

(32) Lenkinski, R. E. In *Biological Magnetic Resonance*; Berliner, L. J.; Reuben, J., Eds.; Plenum: New York, 1984; Vol. 6; p 26.

(33) Murray, L. D.; Touche, D.; Williams, D. R. *J. Chem. Soc., Dalton Trans.* **1976**, 1355.

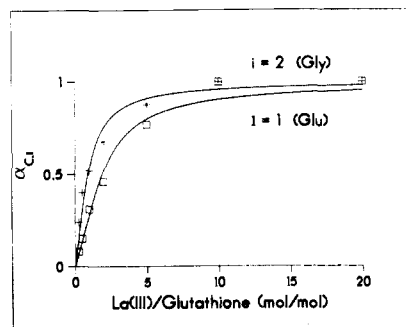


Figure 3. Fractional complexation at the carboxylates of glutathione as a function of added lanthanum(III). Symbols indicate experimental points, and solid lines, the fitted response. See text for definitions.

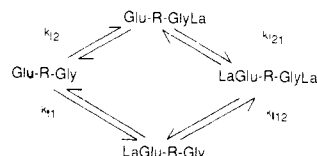


Figure 4. Microscopic complex formation scheme for glutathione. Glu-R-Gly is GSH deprotonated at both carboxylates.

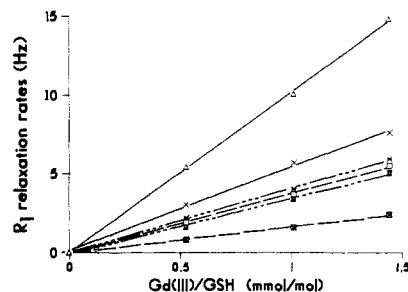


Figure 5. Gd(III)-induced  $^1\text{H}$  NMR relaxation rate enhancement of glutathione:  $\Delta$ , Gly  $\alpha\text{-H}_2$ ;  $\times$ , Glu  $\alpha\text{-H}$ ;  $*$ , Glu  $\beta\text{-H}_2$ ;  $\square$ , Glu  $\gamma\text{-H}_2$ ;  $\text{XX}$ , Cys  $\alpha\text{-H}$ ;  $\blacksquare$ , Cys  $\beta\text{-H}_2$ .

below, this excludes the simultaneous complexation of a lanthanum(III) ion by both carboxylates of one glutathione molecule as a major complexation mode.

We measured the chemical shift of the carboxylate carbons as a function of the La(III)/GSH ratio, to obtain further proof of the competing complexation of the La(III) ion by both the glycine and the glutamic acid carboxylate groups of GSH. From these data, plots of fractional complexation at each site are readily derived (see Figure 3). These can be used to determine the microscopic formation constants at the two sites. The reaction scheme is shown in Figure 4. At pH\* 4.6, where the carboxylate groups are deprotonated and the amino and sulfhydryl groups protonated, no other acid-base forms need be considered. The fractional complexation at site  $i$ ,  $\alpha_{c,i}$ , is given by eq 4 where  $f$ ,  $c$ ,

$$\alpha_{c,i} = (\delta_{\text{obsd},i} - \delta_{f,i}) / (\delta_{c,i} - \delta_{f,i}) \quad i = 1 \text{ (Glu) or } 2 \text{ (Gly)} \quad (4)$$

and obsd refer to free, complexed, and observed, respectively. The  $\alpha_{c,i}$  values at various La(III):GSH ratios can then be fitted to an algebraic model based on figure 4, to yield the four microscopic formation constants. (Since these form a closed cycle, there are actually three independent parameters. Computationally, a fit to  $k_{f2}$ ,  $k_{f12}$ , and the parameter  $a (=k_{f1}/k_{f2} = k_{f21}/k_{f12})$  is most convenient.) The values yielded are  $k_{f1} = 76 \pm 25$ ,  $k_{f2} = 177 \pm 50$ ,  $k_{f21} = 23 \pm 10$ , and  $k_{f12} = 54 \pm 20$  ( $a = 0.43 \pm 0.1$ ). When expressions 5 and 6 are used, the macroscopic constants  $K_{f1}$  and

$$K_{f1} = k_{f1} + k_{f2} \quad (5)$$

$$1/K_{f2} = 1/k_{f12} + 1/k_{f21} \quad (6)$$

$K_{f2}$  are determined as  $252 \pm 56$  and  $16 \pm 7$ , respectively. Agreement with the literature value<sup>33</sup> for  $K_{f1}$  of 222 is therefore well within experimental error.

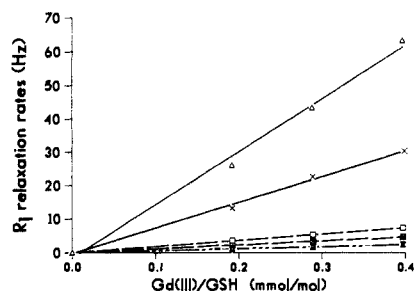


Figure 6. Gd(III)-induced  $^{13}\text{C}$  NMR relaxation rate enhancement of glutathione:  $\Delta$ , Gly COO;  $\times$ , Glu COO;  $\square$ , Gly  $\alpha$ -C;  $\blacksquare$ , Glu  $\alpha$ -C; XX, Glu CON.

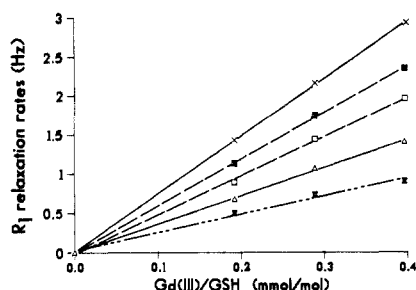


Figure 7. Gd(III)-induced  $^{13}\text{C}$  NMR relaxation rate enhancements of glutathione:  $\times$ , Cys CON;  $\blacksquare$ , Glu  $\beta$ -C;  $\square$ , Glu  $\gamma$ -C;  $\Delta$ , Cys  $\alpha$ -C; XX, Cys  $\beta$ -C.

Very similar conclusions are reached for Gd(III), from observation of GSH in the presence of small amounts of Gd(III). The  $^{13}\text{C}$  spectra display no significant chemical shift differences compared to free GSH (as expected, since Gd(III) is isotropic), but selective line broadenings are observed for different signals (Table III). These are in qualitative agreement with the structures proposed above for the lanthanum(III) complexes. To explore this in more detail, we measured the paramagnetic ion induced  $^1\text{H}$  and  $^{13}\text{C}$  NMR spin-lattice relaxation rates of GSH as a function of the Gd(III)/GSH molar ratio. The results are summarized in Figures 5–7. Consistent with the structures mentioned above, the plots are linear, and their slopes reflect the distance from the sites of complexation. These  $^1\text{H}$  NMR studies were performed under conditions where not more than one Gd(III) ion will be complexed to any given GSH molecule. Assuming that relaxation rates of the protons  $\alpha$  to the complexation sites are the same, the parameter  $a$  can again be estimated. (This implies that Gd–O bond distances are the same at both sites and that coordination to both oxygens is operative. Such has previously been demonstrated to be the case for simpler species.<sup>2</sup> In the present system, the  $^{13}\text{C}$   $T_1$  relaxation rate ratio for carboxylate carbon/ $\alpha$ -carbon at both sites is also very similar (see below). At low Gd(III)/GSH eq 7 is used where  $R_{\text{obsd},i}$  is the observed relaxation

$$R_{\text{obsd},i} = R_{c,i}[\text{ML}]_i/L_t \quad (7)$$

rate,  $R_{c,i}$ , that in the complex, and  $L_t$ , the total ligand concentration. Thus for a given Gd(III)/GSH ratio,  $R_{\text{obsd},1}/R_{\text{obsd},2} = k_{f1}/k_{f2} = a$ . The value obtained is  $0.52 \pm 0.03$ . This analysis is subject to the assumption that not more than one GSH is attached to a given Gd(III) ion; given the excess of GSH in solution, this is questionable. However, provided the microscopic constants at the two carboxylate sites in the second GSH to complex have a similar ratio of complex formation constants to those in the first, the influence upon the measured value will be slight. The close correspondence of this value to that determined for La(III) above, which is not subject to this assumption, supports this.

We can also use the Solomon–Bloembergen equation<sup>18</sup> to extract spatial information. Given certain assumptions, explored in detail previously,<sup>2</sup> relaxation rates in the complex ( $R_c$ ) are proportional to the inverse sixth power of the distance between the nuclei and the paramagnetic ion. A major assumption is that

Table VI. Slopes of the  $^{13}\text{C}$  Relaxation Rates

carbon	measd $R'$ , Hz	calcd $R'$ , Hz
Gly COO	$158000 \pm 9000$	158000
Gly $\alpha$ -C	$18500 \pm 100$	20300
Cys CON	$7390 \pm 50$	4900–8600
Cys $\alpha$ -C	$3600 \pm 80$	2450–8700
Cys $\beta$ -C	$2300 \pm 160$	1760–7900
Glu CON	$5960 \pm 70$	6160
Glu $\gamma$ -C	$4970 \pm 130$	4710
Glu $\beta$ -C	$5950 \pm 60$	4750–7180
Glu $\alpha$ -C	$11700 \pm 200$	10300
Glu COO	$76900 \pm 3500$	76400

<sup>a</sup>Standard deviations are taken from the slopes of the linear regression.

the correlation time characterizing the dipolar interaction upon which relaxation depends is the same for all nuclei under consideration. This is warrantable here because on the basis of theoretically calculated energy maps<sup>7</sup> internal torsional motions will be much slower than the overall rotational motion of the complex as a whole. Under these conditions, for a given complex eq 8 applies, where  $p_j$  is the population of conformer  $j$ ,  $r_j$ , the

$$R_c = C_1 \sum_j (p_j/r_j^6) \quad (8)$$

corresponding distance, and  $C_1$ , a constant. As discussed above, the slopes of the lines of the relaxation rates at different Gd(III) concentrations ( $R'$ ) are proportional to the relaxation rates in the complexes and the relative amount of the two complexes. It can then be shown that eq 9 holds, where the first term describes the

$$R' = C_2 \left[ \sum_j (p_j/r_j^6) + a \sum_k (p_k/r_k^6) \right] \quad (9)$$

effect of the Gd(III) ion complexed to the glycine carboxylate and the second the effect of the Gd(III) ion complexed to the glutamate carboxylate. The term  $a$  allows for the differing degrees of complexation at the two sites.

Table VI shows predicted  $R'$  values according to eq 9. The rotamer populations of Table V determined for the free ligand were used in the calculations and were assumed to be independent of each other. Gd(III)–carbon distances were estimated with the MMS molecular geometry program,<sup>21</sup> with the coordinates of the X-ray structure of glutathione<sup>6</sup> as starting values in the calculations. The Gd(III) ions were located in the structure on the axis of the  $\alpha$ -C–COO bond, at a distance giving an average 350-pm Gd–O bond length and consistent with the best fit to the experimental  $R'_{\text{COO}}/R'_{\alpha\text{-C}}$  ratios. The torsion angles according to the conformations of the free ligand were adjusted, and all the Gd–carbon distances were determined by the program, for all the described stable conformations. Upper and lower limits of the distances were determined in cases where the conformation around  $\chi^3$  affected the value. From the ratio of the  $^{13}\text{C}$   $R'$  values of the carboxylate carbons,  $a$  can again be determined. The value obtained is  $0.49 \pm 0.05$ , in good agreement with the values determined above. According to the MMS molecular modeling, the Gd(III) ion complexed on one end of the molecule in all stable conformations studied is more than 1 nm from the carboxylate and the  $\alpha$ -carbon atoms on the other end, so its relaxation enhancement effects could be neglected. The value of  $C_2$  was determined from regression fits of the calculated data to the measured values for the above-mentioned four carbon atoms and for the Glu  $\gamma$ -C and Glu CON. These  $R'$  values are not affected by the conformational changes around the  $\chi^3$  bond. Predicted ranges of  $R'$  are reported in Table VI for the other carbons, using the upper and lower limits of the determined Gd–carbon distances according to the torsion angle variation around the  $\chi^3$  bond. The experimental  $R'$  values are also given for comparison.

## Discussion

**Conformation of the Free Glutathione.** The true conformation of GSH in aqueous solution is an integral made up of an infinite number of forms, of infinitesimal probability. Our simplified analysis shows, however, that the conformation is by no means

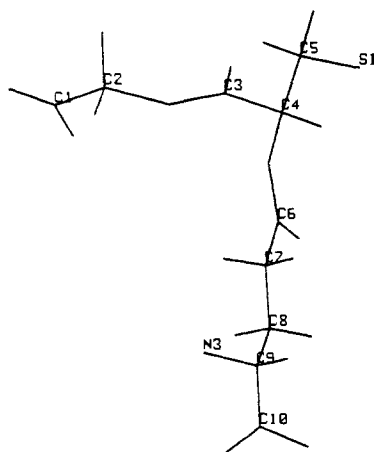


**Figure 8.** Probable conformation of GSH in aqueous solution. C1 is the glycine carboxylate.

random, since not all members of our simplified basis set have equal probability of occurrence. By multiplication of the fractional probabilities of the individual torsion angles that generate a given conformation, the probability of that conformer can be estimated, assuming that the conformational status of one site does not affect conformational probabilities at any other. Figure 8 shows a computer-generated plot of the "most probable conformer"; this, however, still accounts for only 2.3% of GSH conformers. The value expected if conformation were totally random is 0.6%. The earlier studies<sup>16,17</sup> contain partial information regarding side-chain torsion angles. Our values are in agreement where earlier values exist. Table V presents a complete side-chain analysis. It also corrects some minor problems in spectral analysis (for instance, the glutamyl  $\gamma$ -protons are nonequivalent and therefore yield distinct coupling constants).

Agreement with rotamer populations calculated by theoretical methods<sup>7</sup> is also generally quite reasonable, particularly for the bonds characterized by  $\Psi_2$  and  $\phi_2$ . The major exception to this is where theory predicts a five-membered hydrogen-bonded ring conformation, for example involving the glycine moiety (torsion angles  $\Psi_1$  and  $\phi_1$ ). Whereas calculations predict almost complete predominance of this form, the NMR data can be rationalized only if significant contributions from other conformations are included. This effect has been previously noted elsewhere; a recent comparative theoretical and NMR study on the conformation of disubstituted ethanes containing ionized groups<sup>34</sup> noted the same effect and ascribed it to the "neutralizing" effect of the water solvent on the electrostatic interaction of the charged species. The fact that the rate of exchange of the glycine NH with water protons is high<sup>14</sup> also tends to support this conclusion. It should be further noted that for the cysteine moiety the amide NH-water exchange is still faster, and our NMR data predict a still lower population (25%) for this five-membered ring than for the glycine case (36%). Of course, in the cysteine case side-chain inductive effects may also be involved. Because of the many possibilities for hydrogen bonding in GSH, several larger ring conformations have been proposed as significant in the past.<sup>15-17</sup> On the basis of the direct information presented here, it appears that none of these is particularly important, although all those proposed (and others) will contribute to the overall picture. It has already been suggested<sup>17</sup> on the basis of  $T_1$  and nonselective NOE data that one of these has only a transient existence. Glutathione in solution is therefore best visualized as having a pseudorandom conformation, with a slight tendency toward an extended form, and the two small hydrogen-bonded rings alluded to above.

**Structure of the Glutathione-Lanthanide(III) Complexes.** Our data suggest strongly that the conformations of free and lan-

thanide-complexed glutathione are similar. (While it should be realized that the "complexed glutathione" is actually a mixture of species, complexed at two different sites, the likelihood of these having different but compensating conformational behavior, such that the measured coupling constants are unchanged, seems small.) No significant change in the conformation upon Ln(III) complexation to other peptides has been detected in several studies.<sup>35,36</sup> Metal binding is *expected* to alter the conformational situation in some respects; for instance, binding to the glycine carboxylate is expected to lower the extent of hydrogen bonding between this and the amino group. This is not, however, observed; presumably, the difference lies below the definition of the experimental method.

The lanthanum(III)-induced  $^{13}\text{C}$  chemical shift change data clearly indicate that the lanthanide ions coordinate to the two carboxylate groups essentially independently. The  $^{13}\text{C}$  relaxation data similarly show no evidence for chelation of both carboxylates to one Gd(III) ion. The sulfhydryl group, as expected for class A metals, is not involved in complexation; in both the  $^1\text{H}$  and the  $^{13}\text{C}$  work, the lowest relaxation enhancements were observed for the cysteine methylene group.

The fairly interactive microscopic complexation behavior of the GSH carboxylates is interesting, since the present data show that conformations where the two carboxylates are close in space are relatively less probable. In fact, the degree of interaction is similar to that observed for acid dissociation at these sites,<sup>9</sup> consistent with the class A behavior of the lanthanide ions. Since the two carboxylates are separated by 10 bonds, significant interaction through the length of the molecule would appear improbable. It may be that the conformational picture is different for GSH neutralized at one or both carboxylates, a point that could be checked by reinvestigation at lower pH values. Unfortunately, the low-pH data currently available<sup>17</sup> is not complete enough to address this issue.

The  $^{13}\text{C}$  NMR spin-lattice relaxation rates induced by Gd(III) ions give quite a satisfactory fit to our simplified model. The Gd-O bonds are longer in this model than would be expected from X-ray of Gd<sup>III</sup>-carboxylate complexes,<sup>37</sup> a trend previously observed in NMR investigations of amino acid<sup>2</sup> and peptide<sup>36</sup> complexes of Gd(III). The  $^1\text{H}$  relaxation rates could not be fitted to the model because they are all dependent on  $\chi^3$ , but they show the same qualitative trend.

The data clearly indicate that the dominant complexation mode of the Gd(III) ion to a carboxylate group is via a four-membered ring involving the Gd(III) ion and both oxygens of the carboxylate group. This agrees with previous  $^1\text{H}$  NMR studies of amino acids and lactic acid<sup>2</sup> and  $^{13}\text{C}$  NMR studies of hydroxy acids.<sup>38</sup> These showed that very different relative relaxation rates would be expected in the case of other complexation modes such as five-membered ring involving one carboxylate oxygen and the amino nitrogen or via only one carboxylate oxygen. In fact, it was concluded that the amino group tended to reduce the strength of complexation, which is easily rationalized on electrostatic grounds. The present data reinforce this conclusion; the glycine carboxylate of GSH has about twice as high a microscopic complex formation constant as the  $\gamma$ -glutamyl carboxylate, which has a proximate, positively charged amino group.

**Acknowledgment.** We are grateful to the National Sciences and Engineering Research Council of Canada for financial support of this work. Thanks are due also to Dr. Lata Prasad for her help in the MMS calculations.

Registry No. GSH, 70-18-8.

(35) Lenkinski, R. E.; Glickson, J. D. In *Conformation in Biology and Drug Design*; Hruby, V. J., Ed.; The Peptides, Vol. 7; Orlando, FL, 1985; pp 301-353.

(36) Perly, B.; Chachaty, C. *J. Magn. Reson.* **1982**, *49*, 397.

(37) (a) Favas, M. C.; Kepert, D. L.; Skelton, B. W.; White, A. H. *J. Chem. Soc., Dalton Trans.* **1980**, 454. (b) Romanenko, G. V.; Podberezskaya, N. V.; Bakakin, V. *Zh. Strukt. Khim.* **1981**, *11*, 46.

(38) Vijverberg, C. A. M.; Peters, J. A.; Kieboom, A. P. G.; van Bekkum, H. *Tetrahedron* **1986**, *42*, 167.

(34) Abraham, R. J.; Hudson, B. D.; Thomas, W. A. *J. Chem. Soc., Perkin Trans. 2* **1986**, 1635.